A novel material based on an antibacterial choline-calixarene nanoassembly embedded in thin films

Loredana Ferreri[1], Grazia M. L. Consoli[1], Gabriele Clarizia[2], Daniela C. Zampino[3,*] [iD],
Antonia Nostro[4,*], Giuseppe Granata[1], Giovanna Ginestra[4], Maria L. Giuffrida[5],
Stefania Zimbone[5], and Paola Bernardo[2]

[1] *Institute of Biomolecular Chemistry (ICB-CNR), 95126 Catania, Italy*

[2] *Institute On Membrane Technology (ITM-CNR), 87036 Rende, CS, Italy*

[3] *Institute of Polymers, Composites and Biomaterials (IPCB-CNR), Section of Catania, 95126 Catania, Italy*

[4] *Department of Chemical, Biological, Pharmaceutical and Environmental Sciences, University of Messina, 98122 Messina, Italy*

[5] *Institute of Crystallography (IC-CNR), 95126 Catania, Italy*

ABSTRACT

Supramolecular chemistry is one of the current strategies for producing advanced materials. With the aim to develop new Thin-Films with antibacterial activity, we embedded an amphiphilic choline-calix[4]arene possessing antibacterial properties in polymeric Thin-Films based on polyether-co-amide matrix (Pebax®2533). The loading of the calix[4]arene derivative in the film was performed by solution casting. The amount of calixarene additive in the films was in the range of 0.5–5 wt%. The self-supported Thin-Films were characterized by investigating phase miscibility, morphology, spectral properties, and gas transport. The release of the calixarene derivative from the films was studied in a biomimetic medium as PBS (10 mM, pH 7.4). The presence of the additive did not affect the thermal stability of the copolymer, whereas it induced an increase in crystallinity, wettability, and gas permeability of the blend films according to its concentration. The antibacterial activity of the films was evaluated in vitro against *Escherichia coli* and *Staphylococcus aureus* strains, representative of Gram-negative and Gram-positive bacteria. The developed films displayed antibacterial activity against both strains. In particular, Pebax® − 5 wt% Chol-Calix caused within 10 h a reduction in *E. coli* and *S. aureus* of 2.57 and 2 log CFU/mL, respectively. The potential toxicity of the films was also tested on mouse embryonic fibroblasts NIH/3T3. Pebax®2533/calixarene derivative combination appears a promising approach for the development of novel flexible antibacterial materials.
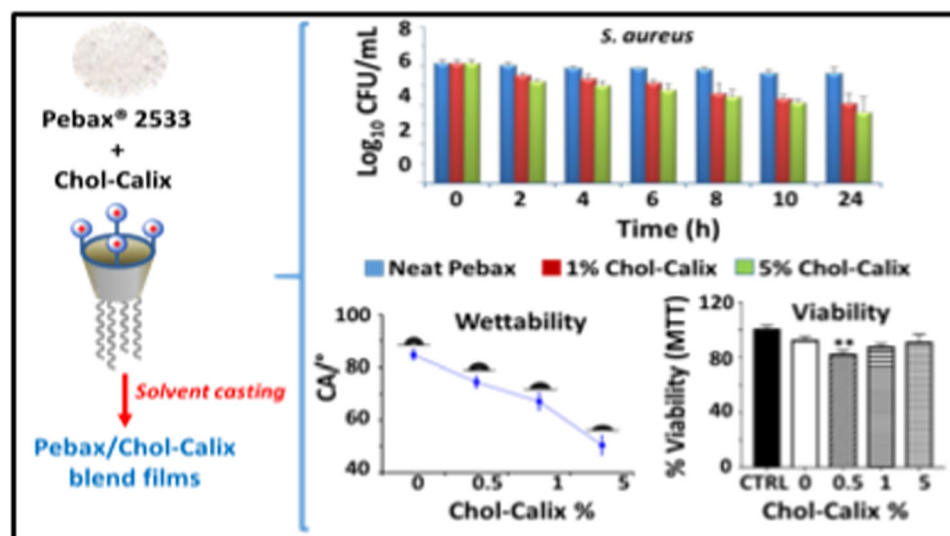
GRAPHICAL ABSTRACT

Introduction

Many areas of our daily life need the control over the microbial contamination, as in food packaging and biomedical devices, to prevent severe threats for public health and safety [1]. High volatility and leaching phenomena affect the traditional low molecular weight disinfectants; therefore antibacterial contact polymers are recently adopted in medical apparatuses, food packaging applications, and water pipe systems by virtue of their long-term stability and absence of toxic residues.

Macrocycle-based antibacterial materials display an effective activity against Gram-negative, Gram-positive, and drug-resistant bacteria [2]. Their action is capable to complement traditional drugs, facilitating the development of modern medicine, and overcoming the antibiotic-resistance emergency. Calix[n]arenes, cyclic compounds with permanent porosity, are macrocycles with hydrophobic cavity interiors and the possibility to functionalize the upper and lower rims, resulting in customized formulations [3]. Small molecules can be complexed within these macrocycles. More fascinating are the self-assembly properties of calixarenes that enable the

production of functional nanomaterials, opening new opportunities for drug delivery of guest biomolecules [4, 5]. Indeed, aggregated nanostructures can be obtained by manipulating calixarene units and exploited as carriers for bio relevant molecules, due to water solubility, low cytotoxicity, and good biocompatibility [6]. Numerous pharmacological properties of calixarenes have also been described, including antibacterial, antifungal, antiviral [7, 8] and anticancer activity [9]. The introduction and spatial orientation of multiple cationic groups on the calix[4]arene scaffold has provided a variety of derivatives with effective antibacterial activity [10].

Among the cationic calix[4]arene derivatives, an amphiphilic derivative (Chol-Calix), bearing choline groups and dodecyl aliphatic chains at the upper and lower rim of a calixarene platform, self-assembles in micellar nanoaggregates with demonstrated properties as gene [11] and drug delivery system [12, 13]. In the search for novel antibacterial agents, we previously demonstrated the potential of Chol-Calix as a nanocarrier for application in antimicrobial photodynamic and photo-induced therapy. The entrapment of a photosensitizer (porphyrin or phthalocyanine derivatives)[14] and/or a nitric oxide photo-donor (*N*-dodecyl-3-(trifluoromethyl)-4-

nitrobenzenamine) [15] in the Chol-Calix micelles resulted in a rapid and effective light-induced antibacterial activity against *Staphylococcus aureus* and *Pseudomonas aeruginosa*. Recently, we demonstrated that the micellar Chol-Calix is also a nanocontainer for conventional antibiotics (ofloxacin, tetracycline, and chloramphenicol) [16] and that it possesses intrinsic antibacterial properties. Indeed, Chol-Calix showed MIC values in the range of 9.4–18.8 µg/mL and inhibited biofilm and mobility of *P. aeruginosa* and *Escherichia coli* strains [17].

Polymeric Thin-Films represent a versatile approach for controlled and localized drug release [18]. Embedding in Thin-Films could be a strategy to expand the range of applications of Chol-Calix, including the achievement of a novel material with antibacterial surface and medical devices enforced with antibacterial activity.

Swell-encapsulation or covalent immobilization are recognized methods to provide successful antimicrobial surfaces [19]. However, solution blending of nanocarriers and selected polymers is low-cost and less time-consuming procedure with respect to polymer grafting that could require multiple surface modification steps. The preparation of gel membranes incorporating Ionic Liquids within a polymeric matrix was successfully carried out using Polyether block amides, commercially available as Pebax® [20, 21]. Pebax are plasticizer-free Thermoplastic Elastomers (TPE) [22]. They are medically relevant polymers commonly adopted to fabricate catheters and medical tubings due to their good kink and chemical resistance. They have been explored for a range of biomedical applications [23] as in the production of breathable films [24], or antimicrobial surfaces incorporating photosensitizers [25]. Being rubbery, Pebax can provide flexible films without requiring harmful plasticizers as typically done with polyvinyl chloride (PVC) which is widely used for medical devices [26, 27].

In this work, we encapsulated Chol-Calix within a polymer matrix in order to produce novel flexible antibacterial materials. For immobilizing Chol-Calix into a Pebax® copolymer, we adopted the solvent-casting method. A polymeric solution was obtained by using a solvent capable to dissolve both the polymer and the additive. Owing to the Chol-Calix solubility in alcohols, the hydrophobic Pebax® 2533 grade that can be dissolved in different alcohols was selected [28]. In the solvent solution, the polymer chains are extended, allowing the encapsulation of the complexes, while after the solvent evaporation the polymer entanglements trap the Chol-Calix.

The antibacterial activity of the prepared films was assessed against specimens of Gram negative (*E. coli*) and Gram positive (*S. aureus*) bacteria that represent clinically important strains with an active role in skin wound and nosocomial infections. Wettability, permeation to gases, thermal properties, and Chol-Calix release were evaluated on the filled films for complete characterization. Finally, mouse embryonic fibroblasts NIH/3T3 were exposed to Pebax® Chol-Calix blend films to exclude the potential toxicity of the Chol-Calix released.

Experimental

Materials

All materials for Chol-Calix synthesis were purchased from Sigma-Aldrich (Milan, Italy) and used without further purification. The block copolymer Pebax® 2533 was received in pellets from Arkema, Italy. The flexible polyether phase is predominant in this copolymer grade (80%). Ethanol (absolute, VWR, Italy) was used as a solvent for preparing the membranes. Gases used for tests were: He, O_2, N_2, CH_4 and CO_2 (purity of 99.99 + %) from SAPIO, Italy. Tryptone Soya Agar (TSA) and Luria–Bertani Broth (LB) were purchased from Difco (Italy), 3-(4,5-dimethylthiazol-2-yl)-2,5-diphenyltetrazolium bromide (MTT) was bought from Sigma-Aldrich (Milan, Italy).

Chol-calix synthesis

Chol-Calix was synthesized by adapting a reported procedure [12]. Briefly, to a solution of tetrachloromethyl-*O*-dodecyl calix[4]arene [29] (4.1 g, 3.2 mmol) dissolved in THF (60 mL), a solution of *N,N*-dimethylethanolamine (1.5 mL, 14.9 mmol) in THF (15 mL) was added. The reaction mixture was refluxed for 24 h. After cooling, the suspension was centrifuged at 4000 rpm for 5 min. The precipitate was washed with THF (40 mL) and then with acetonitrile (4 × 20 mL) by repeated centrifugation (4000 rpm, 5 min) and removal of the solvent. The precipitate was dried under vacuum to give a white powder (4.2 g, 80% yield). The obtained Chol-Calix

(MW 1648.2 for $C_{96}H_{168}Cl_4N_4O_8$) was characterized by NMR spectroscopy and the spectral data were consistent with those reported in the literature [16, 17].

Membrane preparation

The Pebax® 2533 pellets were dissolved into ethanol at a concentration of 3 wt% under reflux conditions for ca. 2 h. Being non-toxic, ethanol was preferred to other alcohols such as methanol and isopropyl alcohol that display similar solvent strength, polarity and hydrogen bonding ability [30]. Weighted amounts of the additive were introduced into the cooled polymer solution to avoid any thermal degradation and damage of Chol-Calix. The resulting solution was left under stirring before its casting. Dense Thin-Films were prepared according to a controlled solvent evaporation procedure, pouring fixed amounts of the dope solution within a stainless-steel ring on a Teflon support. After the evaporation of the solvent, the films were detached from the plate and cut for the characterization. The resulting samples contained 0.5, 1 and 5 wt% of Chol-Calix. Isotropic films based on the neat polymer were prepared as well and used as reference.

Characterization

Fourier transform infrared spectroscopy (FTIR)

Functional groups of the prepared films were investigated by Attenuated Total Reflection (ATR) FTIR analysis (Spectrum One, Perkin Elmer). The spectra were recorded in the region from 4000 to 650 cm^{-1}, with a resolution of 4 cm^{-1} (16 scans).

Thermal analysis

Calorimetric measurements of neat polymer and Chol-Calix blend films were conducted using a differential scanning calorimeter (DSC, TA Instruments Q100), equipped with a liquid sub ambient accessory. High purity standards (indium and cyclohexane) were used for calibration. All DSC runs were carried out at a rate of 10 °C/min from − 90 to 250 °C using nitrogen as purge gas. Sample weight was in the range 4–6 mg. Heating and cooling scans were performed after an initial equilibration to − 90 °C. To erase the previous thermal history, a first heating scan from − 90 °C to 250 °C was made. Then a cooling run (from 250 °C to − 90 °C) and a second heating one (from − 90 °C to 250 °C) were executed.

Thermogravimetric analysis (TGA) was carried out using a thermogravimetric apparatus (TGA, TA Instruments Q500) under a nitrogen atmosphere at 10 °C/min heating rate, from 40 to 600 °C. Dried samples of about 4–6 mg were put into a platinum pan. TGA data and their derivative (DTG) ones were recorded as a function of temperature.

Gas permeation tests

Permeation properties of the prepared films were measured at 25 °C. Circular samples with an effective area of 11.3 cm^2 were used. Their thickness was measured using a digital micrometer (IP65, Mitutoyo), considering the average of multiple point measurements.

The testing apparatus is a constant-volume/variable-pressure device described elsewhere [28]. Before each test, the films were thoroughly evacuated using a turbomolecular pump to remove eventually dissolved species (e.g., residual solvent, humidity, previously tested gases). The data, obtained measuring the increasing gas pressure signal in the permeate side *vs.* time, were elaborated according to the time-lag method, evaluating the permeability (P) as well as the diffusion coefficient (D) of each gas through the membrane [31] considering the "solution-diffusion" model that describes the transport in dense polymeric films [32].

Scanning electron microscopy (SEM)

Samples for SEM analysis were prepared by sputter-coating with a thin film of gold. Gold sputtering thickness was about 5 nm. Sample images were acquired on a JEOL (JXA-8230 SuperProbe Electron Probe Microanalyzer) SEM operated at 20 kV.

Water contact angle analysis

Static water contact angle (WCA) measurements were determined using a DATAPHYSICS OCA 15EC apparatus and water as liquid. Specifically, a drop (2 μL) of deionized water was deposited on the sample surface and the measurement was made after

its stabilization ($\sim$ 10 s). Three measurements on different areas of each sample were executed. WCA results are average values ($\pm$ 1–3° standard deviation) of triplicate samples.

Release of Chol-Calix from the blend films

The release kinetics of Chol-Calix from the films (0.5, 1, 5 wt%) was determined by immersing a rectangular sample (5 mg, thickness 80 µm, size 7 × 10 mm) in 3 mL of PBS. The samples with and without Chol-Calix were kept at 37 °C; then, at specific interval times, the optical absorption at 210 nm was measured. By subtracting the absorption of the neat sample, the absorbances of the Pebax®/Chol-Calix samples were converted to the amount of Chol-Calix released, based on a calibration curve. The absorption spectra were recorded on a Jasco V-770 spectrophotometer. The release data were fitted (coefficient of determination, R^2 = 0.999) by the following exponential function:

$$R(\%) = R(\%)_{max} \cdot \left(1 - e^{-kt}\right)$$

where $R(\%)$ is the release percentage at time t, $R(\%)_{max}$ is the maximum release percentage and k the first order kinetic constant. Indeed, first-order equations well describe the dissolution of water-soluble drug from porous matrices [33]. The release experiments were performed in triplicate.

To simulate the conditions of the antibacterial assays, the release of Chol-Calix from the Pebax® blend films was also investigated on larger samples (2 cm diameter, 32 mg, 80 µm) immersed in 1 mL of PBS for 24 h.

Antibacterial activity and biofilm biomass measurement

Test organisms used in this study were *E. coli* ATCC 10536 and *S. aureus* ATCC 6538. For the antibacterial tests, the cultures were grown overnight on LB and washed in phosphate buffered saline (PBS, pH 7.2) by centrifugation at 3500 rpm for 15 min and adjusted to a concentration of 5 × 10^5–1 × 10^6 CFU/mL, approximatively. The standardized cultures (1 mL) were dispensed into each well of a 12-well cell culture treated polystyrene microtiter plate. The different polymeric films (round samples, 2 cm in diameter, 32 mg, 80 µm), neat (control) or with Chol-Calix at various concentrations (0.5, 1, 5 wt%) were then

placed in each well of the microtiter plate. After incubation at 37 °C for different time intervals (2, 4, 6, 8, 10 and 24 h), the planktonic phase was serially diluted in PBS, plated onto TSA and incubated for 24–48 h at 37 °C in order to evaluate the number of CFU/mL. All the determinations were performed in triplicate including the growth controls.

Moreover, after 24 h-incubation the biofilm formed on the polymeric films with Chol-Calix at 5 wt% was evaluated by biomass measurement. The polymeric films were washed twice with PBS, dried, stained for 1 min with 0.1% safranin, and then washed with water as previously reported [34]. The stained biofilms were suspended in 30% acetic acid aqueous solution and the mean optical density at 492 nm (OD_{492}) was measured using a spectrophotometer EIA reader (Bio-Rad Model 2550, Richmond, CA, USA). The reduction percentage of biofilm was calculated using the following equation:

$$\text{Biofilm Reduction} (\%) = 100 - \frac{OD_{492}\ \text{Pebax}^®/\text{CholCalix}}{OD_{492}\ \text{neat Pebax}^®} \times 100$$

The films were sterilized under a UV lamp (256 nm) for 5 min before each assay.

Cell viability

Cell culture

The mouse embryonic fibroblasts NIH/3T3, purchased from ATCC cells bank (CRL-1658), were maintained in DMEM-F12 (Gibco, Thermofisher) supplemented with 10% heat-inactivated (HI) fetal bovine serum (Gibco, Thermofisher), 100 mg/mL penicillin, and streptomycin (Gibco, Thermofisher), and 2 mM L-glutamine at 37 °C, 5% CO_2. NIH/3T3 cells for the performed experiments were used at passage 7–9. One day before experiments, 25 × 10^3 cells were plated on 96 multi-well plates in DMEM-F12 with 5% fetal calf serum (FCS).

Before treatments, cells were washed with phosphate-buffered saline (PBS) and the medium was replaced with fresh DMEM F-12 with 5% FCS.

Cytotoxicity test

To test the potential cytotoxicity of the Pebax®/Chol-Calix blend films, we studied the effect of the Chol-Calix released from differently loaded films according to the MTT assay. N = 9 round samples (3 mm in

diameter, 3 mg in weight) of neat Pebax® and its films containing 0.5, 1, and 5% of Chol-Calix, were firstly kept for 5 min under UV lamp to sterilize them, thus avoiding cellular contamination. Then they were incubated in 100 μL of 5% FBS DMEM/F12 for 4 h at 37 °C in separated wells of a 96well-microplate, the fibroblasts were washed with PBS and the medium was replaced with those containing the released compounds (100 μL). After 48 h of treatments, we added 20 μL of MTT (0.5 mg/mL) to each well for 2 h at 37 °C, then the medium was discarded and the water-insoluble formazan crystals were dissolved in DMSO. The formazan production due to the conversion of MTT by living cells, was evaluated in a microplate reader (Varioskan® Flash Spectral Scanning Multimode Readers, Thermo Scientific, Waltham, MA, USA) by reading the absorbance at 570 nm.

Results and discussion

Chol-calix structure and Pebax® blend films preparation

The chemical structure and a schematic representation of Chol-Calix are shown in Fig. 1. As previously reported [15], Dynamic Light Scattering measurements and TEM images showed that Chol-Calix self-assembles in micellar nanoaggregates (46 nm diameter) with a positively charged surface (Z potential $\zeta = + 24.7$ mV) in PBS medium [16].

Flexible free-standing films were obtained without using plasticizers as commonly done with other polymers such as PVC. The blend films were transparent at low concentrations (0.5 and 1 wt%) of Chol-Calix, whereas its incorporation into Pebax® matrix at higher content (5 wt%) induced the formation of a white pigmentation with several small aggregates.

FT-IR analysis

Structural characteristics of pure Pebax® and Chol-Calix-loaded samples were investigated by using the FT-IR analysis. The spectra are shown in Fig. 2.

The neat Pebax® 2533 film displayed strong bands at ca. 1100, 1640, and 3300 cm^{-1}, assigned to the C–O–C (ether group) stretching vibrations within the PTMO block, the H–N–C=O stretching vibrations, and the N–H– stretching vibrations in the polyamide
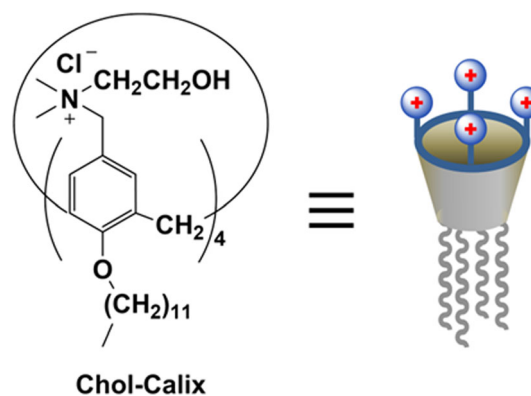

Figure 1 Chemical structure and schematic representation of Chol-Calix.

block, respectively. Other characteristic bands for pure Pebax® membrane are at around 1732 and 2854 cm^{-1} and correspond to the stretching vibrations of C=O and –CH$_3$ groups, while the band at 886 cm^{-1} in the fingerprint region is attributed to the –OH terminal groups in the copolymer (Fig. 2A) [35].

The new band at 1482 cm^{-1} in the blends is typically assigned to the (CH$_3$)$_3$ N$^+$ of choline [36], while that at 1288 cm^{-1} is indicative of the aromatic ring in calixarene (Fig. 3b). The band at 886 cm^{-1} is reduced in the blends, suggesting the interaction of the polymer ends with the additive. The C–O–O– stretch at 816 cm^{-1} in the neat copolymer has a redshift in the blends indicating a weaker bond. The double peak at 1463 cm^{-1} due to the C=O stretching vibration in carbonyl (hydrogen-bonded and free state at higher wavelength) has a more intense bonded part in the blends. The same behavior is observable for the peak at 1563 cm^{-1} that is related to the C–N amide II stretching (Fig. 2B).

Thermal properties

To evaluate the thermal properties and stability of neat Pebax® and Pebax®-Chol-Calix films, DSC and TGA measurements were carried out.

DSC

The thermal properties of the prepared films were investigated by DSC analysis in the temperature range from − 90 to 250 °C. Figure 3 shows the thermograms acquired on the first heating, cooling, and second heating scans for DSC analysis of neat Pebax® and the blends. Two main melting peaks related to

Figure 3 DSC curves of Pebax® and Pebax®-Chol-Calix blends. ▶ (**a**) first heating cycle, (**b**) cooling cycle, (**c**) second heating scans.

both PTMO and PA12 blocks are evident, proving the microphase separated structure of the block copolymer. The analysis of thermograms reported in Fig. 3 highlights during the first heating run the presence of a main melting peak (T_m) at around 15–16 °C and a second one at ca. 48–49 °C in the PTMO domain of all samples, whereas that of PA12 was at 143 °C for neat Pebax®. This PA12 block peak slightly shifts to higher temperatures (145–148 °C) in the blends. Data of T_m
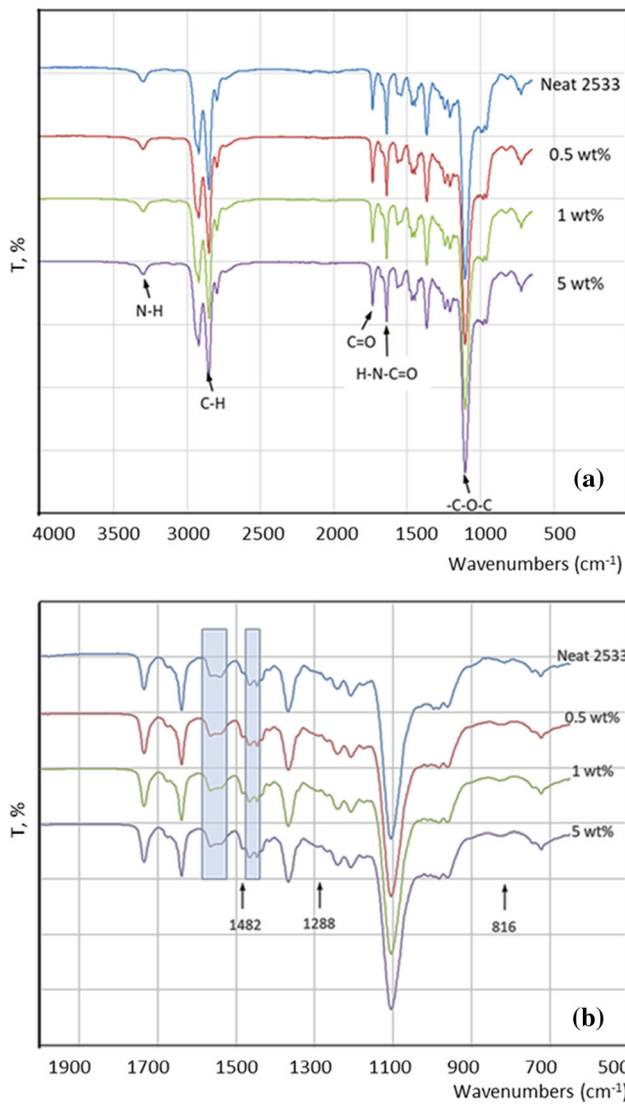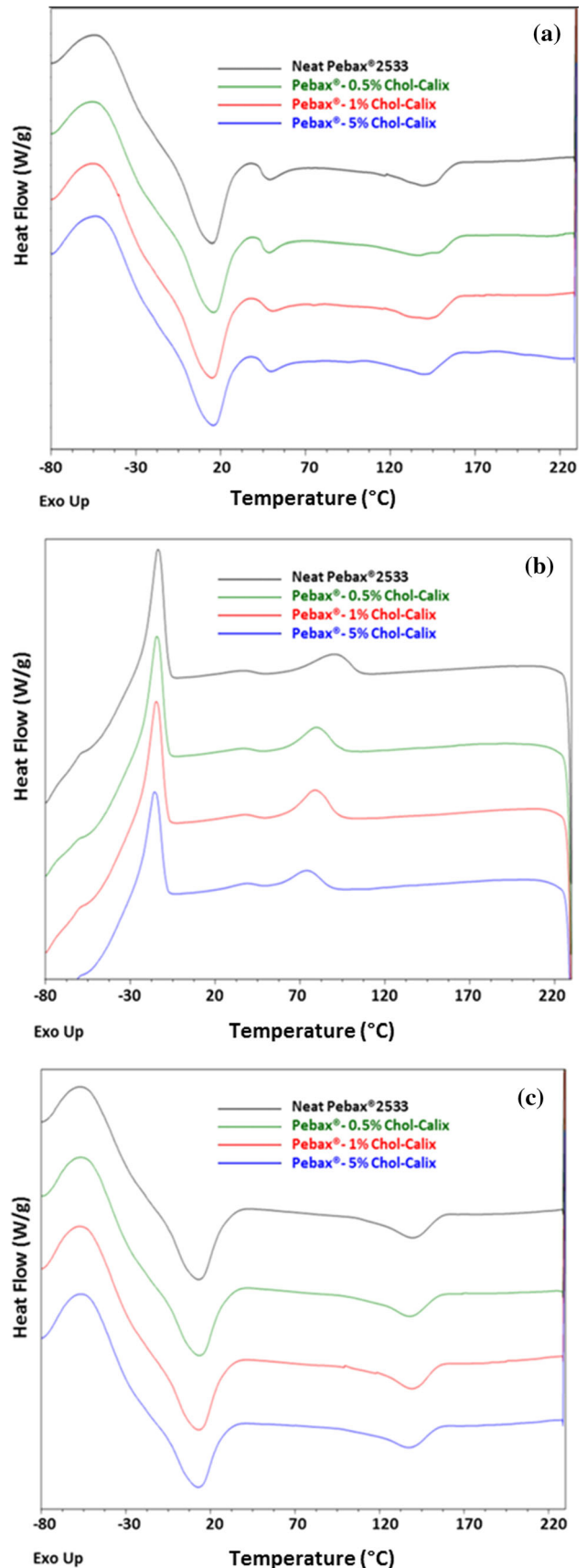

Figure 2 FTIR-ATR spectra of (**a**) Pebax®-based films in the range 500–4000 cm^{-1}, (**b**) enlarged portion of Pebax®-based films in the range 500–2000 cm^{-1}. Transmittance versus wavenumber (cm^{-1}).

and enthalpy of fusion (ΔH_m) together with T_c and enthalpy of crystallization (ΔH_c) of both PTMO and PA blocks in the cooling and second heating runs of neat Pebax® and Pebax®/Chol-Calix blends are reported in Table 1. During the second heating scan, the PTMO melting peak at ca. 48–49 °C, probably due to a kinetically less favorable crystal phase induced by the slow solvent evaporation, disappears in all samples, whereas the main T_m peak shows a slight decrease to lower temperatures (13–14 °C) for neat Pebax® and its blends, respectively. Likewise, the T_m peak of PA12 domain shifts to lower temperatures (140–141.5 °C) in all samples (Fig. 3, Table 1). During both heating scans, it is possible to observe a broad glass transition (T_g) at around − 38 °C that starts at ca. − 48 °C and ends at − 28 °C in all samples, with no differences between neat polymer and its blends. This T_g value is higher than that previously observed [37], detected at temperature below − 50 °C.

During the cooling cycle, the PTMO domain shows a slight increase in both T_c and ΔH_c from − 16 and 22 °C (neat Pebax®) to − 14 and 27 °C (Pebax®-− 5wt% Chol-Calix blend), respectively. As well a similar increase was noted in the PA domain, with T_c and ΔH_c values ranging from 75 and 5.0 °C (neat Pebax®) to 91 and 7.0 °C (Pebax® − 5 wt% Chol-Calix blend), suggesting that crystallinity of blends is additive dose-dependent. In general, Chol-Calix addition into Pebax®2533 matrix does not influence the position of melting peaks in both polyether and polyamide domains, whereas this addition causes a slight crystallization shift to higher temperatures, more evident in the PA domain. According to Table 1, the crystallinity increased for both Pebax domains upon the additive loading, particularly for the hard polyamide block. DSC data suggest phase separation between polymer matrix and additive, more evident at the higher Chol-Calix concentration (that aggregates/migrates on the polymer surface, as demonstrated by SEM and WCA results).

TGA

Thermogravimetric analyses were performed in the temperature range of degradation from 40 to 600 °C. TGA ramped experiments with a 10 °C/min heating rate were carried out to obtain reliable results on thermal stability of neat Pebax® and its blends, comparable with those of literature data [21]. A platinum pan and nitrogen gas were used to avoid degradation differences caused by different pan and gas types, respectively. We considered as T_{onset} the temperature at 5% weight loss to prevent the uncertainty from the manually determination of the T_{onset} tangent point. The thermogram overlays and DTG curves of neat Pebax® and its blends are shown in Fig. 4. The mass losses (TG) at 5% and 50%, the decomposition maximum temperature of thermal degradation (T_d) and the weight residue (%) at 600 °C are reported in Table 2.

The neat Pebax® and the Chol-Calix loaded films displayed a single step degradation, regarding the random chain scission mechanism of the main polymer chain and corresponding to 50% weight loss. The maximum degradation temperatures were at about 423 °C and at 422–420 °C for the neat Pebax® and for the blend films, respectively. A decrease in T_{onset} of polymer blends was observed. In particular, Pebax® − 5wt% Chol-Calix sample showed a 20 °C decrease in T_{onset} with respect to that of neat Pebax® as previously reported with the loading of other antibacterial additives (long chain imidazolium Ionic

Table 1 Glass transition temperature (T_g), melting (T_m) and crystallization (T_c) temperatures, enthalpy of fusion (ΔH_m) and enthalpy of crystallization (ΔH_c) of PTMO and PA blocks in the cooling and second heating scans of neat Pebax® and its blends

Sample	Cooling				II Heating				
	Polyether domain		Polyamide domain		Polyether domain			Polyamide domain	
	T_c (°C)	ΔH_c (J/g.)	T_c (°C)	ΔH_c (J/g.)	T_g (°C)	T_m (°C)	ΔH_m (J/g.)	T_m (°C)	ΔH_m (J/g.)
Neat Pebax®2533	− 16.0	22.15	75.2	5.02	− 37.8	13.0	16.48	140.3	2.84
Pebax® − 0.5 wt% Chol-Calix	− 15.0	26.17	79.2	7.84	− 39.2	13.6	17.60	140.8	4.59
Pebax® − 1 wt% Chol-Calix	− 14.5	25.02	80.2	7.43	− 37.9	14.0	17.37	140.0	3.81
Pebax® − 5 wt% Chol-Calix	− 13.9	27.21	90.8	7.32	− 38.4	13.5	17.71	141.5	3.89

Figure 4 Thermogravimetric curves of Pebax® and Pebax®/Chol-Calix blends. In the inset the DGT curves.
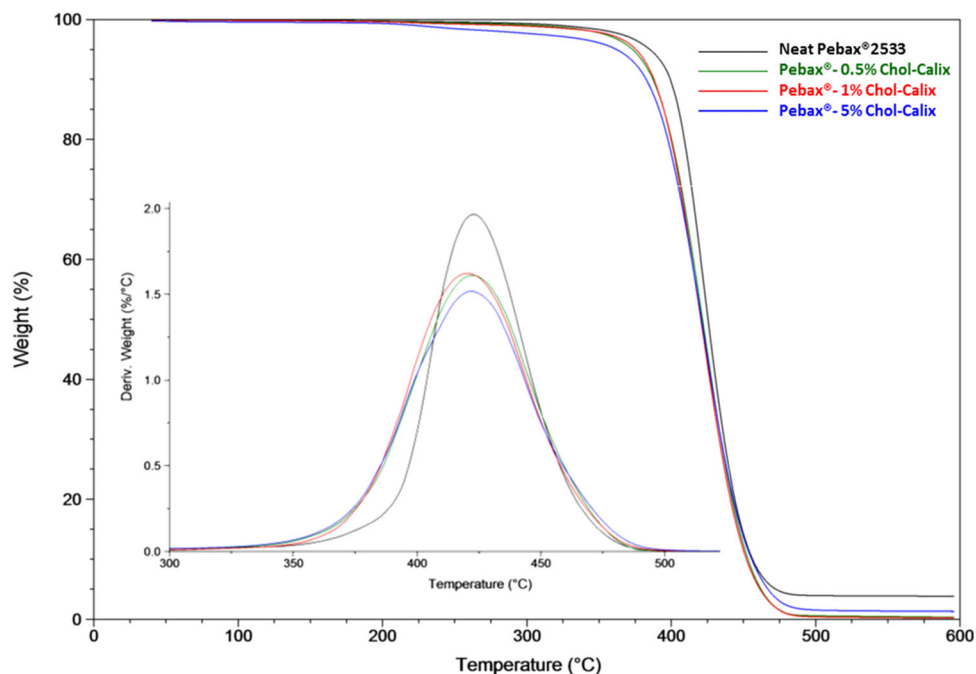
Liquids) into a Pebax® matrix [21]. Nevertheless, the thermograms evidenced that the presence of Chol-Calix does not influence the thermal degradation pattern of the polymer, because no significant differences between neat Pebax® and polymer blends were observed at onset temperature below 350 °C, confirming the thermal stability of polymer and its blends. This was also confirmed by the degradation temperature, T_d, that was not influenced by the addition of Chol-Calix into Pebax®Rnew matrix, displaying values (420–422 °C) very similar to that of neat polymer (423 °C) in all blend samples.

The residue of blends is less than that of neat polymer, confirming the almost total degradation of the samples at 600 °C.

Gas permeation measurements

To verify the integrity of the prepared films, single gas permeation tests were carried out. The permeation parameters of the samples are reported in Figs. 6 and 7. The addition of Chol-Calix at a low concentration (0.5 wt%) depressed the gas permeability of the polymer matrix. This is the typical behavior of impermeable fillers that can be predicted by a Maxwell model [38]. At the same time, the reduced gas permeability reflects the larger crystallinity in the copolymer evidenced by DSC. However, the microstructure of the Thin-Films is composition-dependent. The larger permeability measured on the films loaded with 1 wt% of Chol-Calix indicates the initial formation of filler aggregates that becomes more significant at a concentration of 5 wt% of Chol-Calix. As a consequence of this phenomenon, a decrease in gas permselectivity with respect to the neat polymer membranes was observed (Fig. 5). Indeed, depending on the filler type and composition, once above a threshold loading, the fillers start to agglomerate with negative effects on the gas separation performance of the membranes [39].

However, the permeation rate order for the different gases in the neat copolymer is maintained in the loaded films: CO_2 is the most permeable species among the tested gases, whereas N_2 is the lowest one. Methane is more permeable than helium, which results faster than O_2. Only in the case of the more concentrated samples (5 wt%), a Knudsen-type mechanism becomes concurrent with the dominant solution-diffusion one, justifying the significant decrease in gas permselectivity (Fig. 5). Gas diffusion coefficients follow the same trend observed for the gas permeability, as function of the filler loading. Indeed, after a generalized decrease for the samples containing 0.5 wt% of Chol-Calix, the diffusion coefficients increase as the filler concentration rises. The diffusion order is the following in both neat polymer and loaded films:

Table 2 Thermogravimetric data of neat Pebax® and its blends

Sample	$T_{\Delta m = 5\%}$ (°C)[a]	$T_{\Delta m = 50\%}$ (°C)[b]	T_d (°C)[c]	% R[d]
Neat Pebax® 2533	385.0	425.5	422.7	3.80
Pebax® − 0.5 wt% Chol-Calix	381.0	421.9	422.0	0.23
Pebax® − 1 wt% Chol-Calix	378.5	421.3	421.2	0.30
Pebax® − 5 wt% Chol-Calix	365.0	419.3	419.7	0.52

[a]Onset of degradation (temperature of 5% weight loss)

[b]Onset of degradation (temperature of 50% weight loss)

[c]Decomposition maximum temperature of thermal degradation

[d]Weight residue (%) at 600 °C
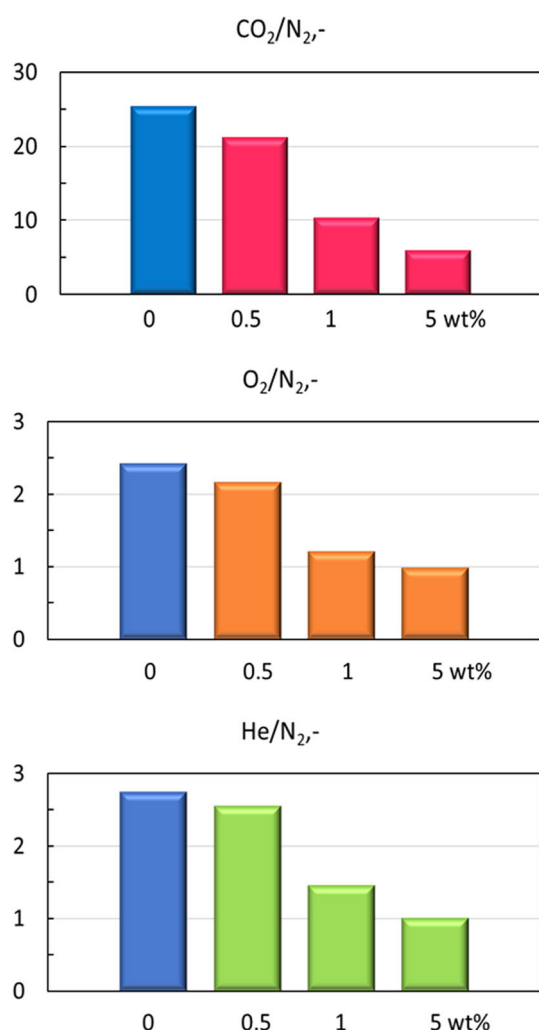
Figure 5 Gas permselectivity of Pebax®-based films measured at 25 °C.

$He > O_2 > N_2 > CO_2 > CH_4$, according to the increasing gas molecular size.

Consequently, the highest permeability measured for CO_2 depends on its larger solubility contribution in polymer matrix. This term also justifies the lower percentage permeability increase measured for CO_2, upon filler addition, with respect to the other gases (Fig. 6).

Surface morphology

Scanning electron microscopy (SEM) was acquired on the surface of the prepared films (Fig. 7). As filler concentration increases, the surface roughness rises. At a Chol-Calix concentration of 5 wt%, a decrease in compatibility with the polymer matrix was experienced determining a surface segregation with the formation of microstructures with sizes ranging from 180 to 310 nm. Information collected by SEM analysis supported the WCA measurements as discussed below.

Surface wettability

The effect of adding different weight percent (0.5, 1, 5) of Chol-Calix on surface wettability of Pebax® blends was investigated. The WCA measured on the prepared films is shown in Fig. 8. The unloaded Pebax® is a hydrophobic material (84.8°), whereas Pebax® blend films loaded with Chol-Calix are hydrophilic. Indeed, due to the presence of quaternary ammonium groups, Chol-Calix nanoaggregates possess a positively charged surface with a zeta potential of + 24.7 mV. The addition of Chol-Calix induced a reduction in WCA with respect to neat polymer, depending on additive content. In particular, when the Chol-Calix concentration increased up to 5 wt%, the contact angle values of the treated Pebax® films decreased from 84.8° to 50.4°, while the loading in Pebax® matrix of lower Chol-Calix contents induced a minor decrease in WCA values, from 84.8° to 74.6° (0.5 wt%) and to 67.2° (1 wt%). This indicates that Chol-Calix concentration into Pebax®

Figure 6 Gas permeability of Pebax®-based films measured at 25 °C and percentage variation of permeability in the loaded films with respect to the neat polymer (P/P₀). 1 Barrer = 10^{-10} cm³ (STP) cm cm⁻² cmHg⁻¹ s⁻¹.
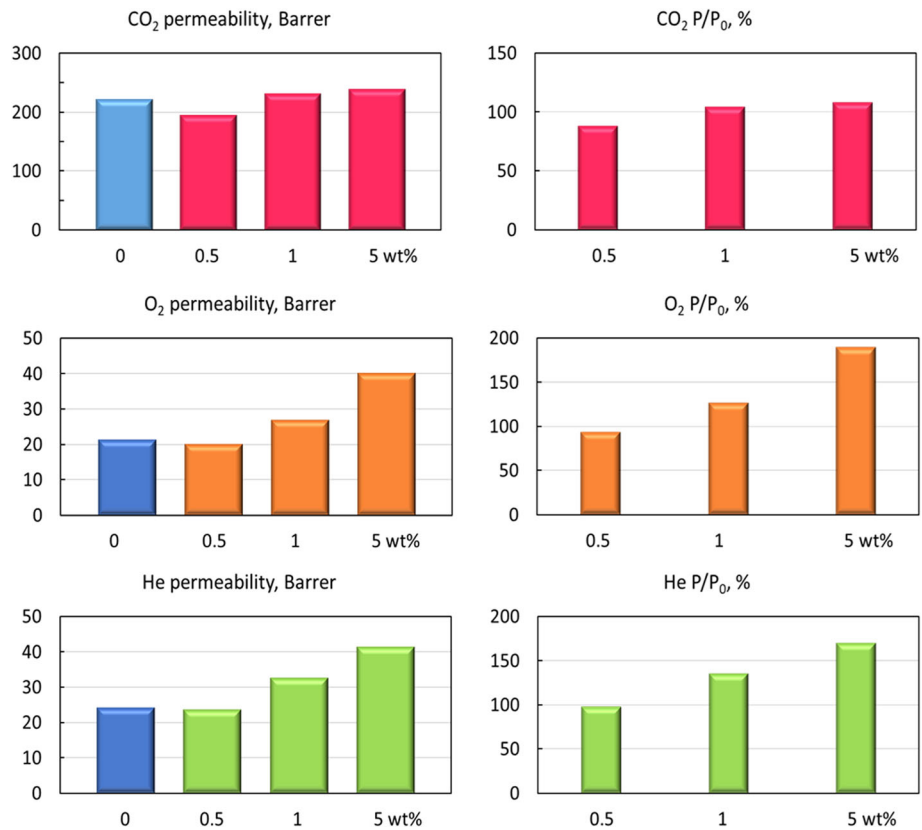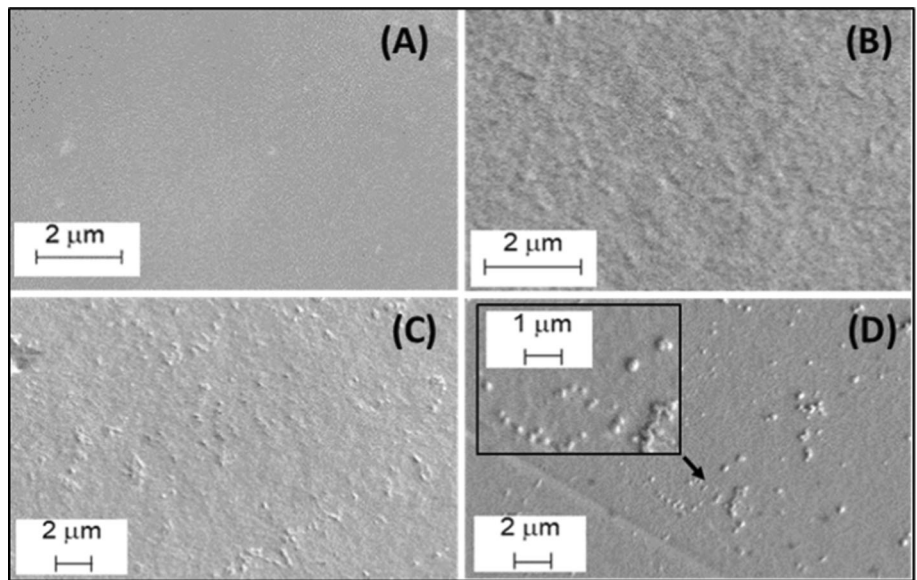

Figure 7 SEM images of the film surface of **A** neat Pebax®, **B** Pebax® − 0.5% Chol-Calix, **C** Pebax® − 1% Chol-Calix and **D** Pebax® − 5% Chol-Calix. Images magnification 10 000 × . Inset magnification 20 000 × .

blends is decisive for surface wettability, with the higher concentration (5 wt%) that induces polymer hydrophilicity. A less homogeneous surface at the higher content (5 wt%) of Chol-Calix, characterized by microstructures, as testified by SEM images, is also responsible for the high standard deviation in the measurements (4–5°).

We suppose that a specific orientation of the hydrophobic side chains toward the Pebax® matrix and of the hydrophilic quaternary ammonium groups towards the polymer surface could occur, as
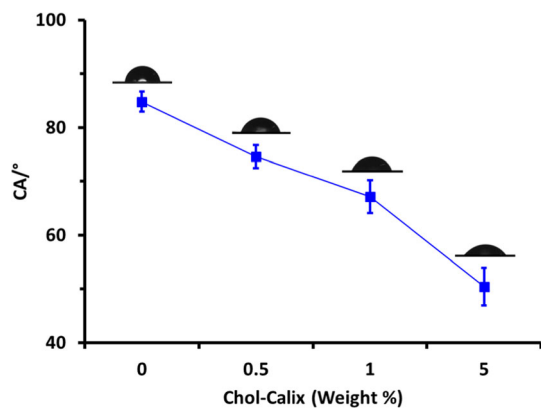
Figure 8 Water contact angle of Pebax® blends as function of Chol-Calix weight percent.

Figure 9 Release (%) of Chol-Calix from Pebax® − 5 wt% Chol-Calix film. The dashed red curve was obtained by fitting the release data.

previously observed in Pebax®Rnew and in PVC loaded with different concentrations of Ionic Liquids bearing long alkyl chains on the imidazolium ring in the cation [21, 40].

Chol-calix release

The release of Chol-Calix from the polymeric films in PBS medium was investigated by UV–vis spectrophotometry. As shown in Fig. 9, a rapid release was found for the film loaded with 5 wt% Chol-Calix, reaching a value of 35% within 2 h. No further significant release was observed up to 72 h. Therefore, a large amount of Chol-Calix gets trapped in the film where it establishes weak interactions with the polymer as corroborated by FT-IR spectra. As a confirmation, the Chol-Calix retained in the film (more than 60%) was extracted by MeOH and quantified in the same solvent by optical absorption referring to a calibration curve.

The release profile shown in Fig. 9 is consistent with a first-order release kinetic. The $R(\%)_{max}$ was calculated to be 34.8% and k 3.9 · 10^{-2} min^{-1}. Typically, a first-order kinetic equation describes dissolution of a drug not effectively enclosed in a polymeric matrix and ready to dissolve from the surface [41]. This agreed with the release behavior observed for the films containing Chol-Calix at lower concentration (0.5 and 1 wt%). Indeed, no significant release was observed from the Pebax® − 0.5 wt% Chol-Calix up to 24 h, and a low release of around 3% was observed within 30 min from the Pebax® − 1 wt% Chol-Calix blend without significant further release up to 24 h. Probably, in the samples loaded with lower amounts of Chol-Calix, the drug is more
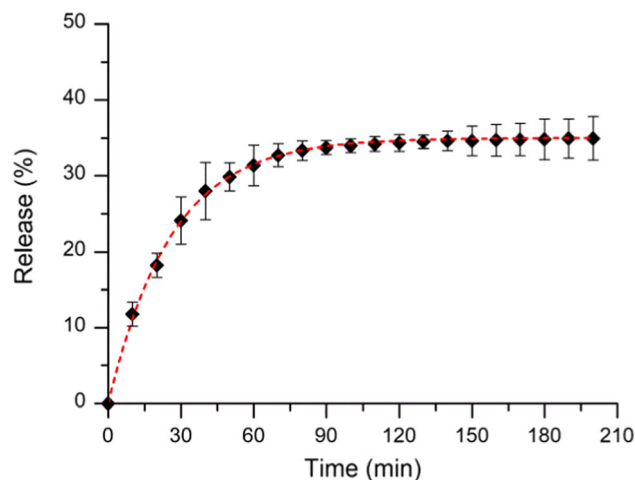
embedded in the films and only a low amount is located on the surface to be released, as evidenced by the SEM images.

The release behavior indicated an accumulation of Chol-Calix on polymer blend surface and it was consistent with WCA data, showing a hydrophilic blend surface. This aspect could be attractive for preventing bacterial growth and hindering bacterial biofilm formation on a material surface [42].

Antibacterial activity

In vitro antibacterial activity was assessed against Gram-negative *E. coli* and Gram-positive *S. aureus*. The results evidenced a relationship between the bacterial growth inhibition and the Chol-Calix concentration (Fig. 10). Neat Pebax® and Pebax® 0.5 wt% showed no significant antibacterial activity within the tested incubation time (24 h) on both *E. coli* and *S. aureus*. This behavior agreed with the absence of antibacterial activity reported for Pebax® 2253 against *S. aureus* and *E. coli* [23] and with the undetectable release of Chol-Calix from the Pebax® − 0.5 wt% film. The Pebax® − 1 wt% Chol-Calix films showed good antibacterial activity against *S. aureus*, with reductions of 1.8 log CFU/mL (98.5% decrease) and 2.1 (99.1% decrease) observed at 10 and 24 h, respectively. Differently, no antibacterial effect was found against *E. coli* consistently with a MIC value (18.8 μg/mL) [17] higher than the amount of the Chol-Calix released from the film (around 10 μg/mL). A clear antibacterial effect was instead observed
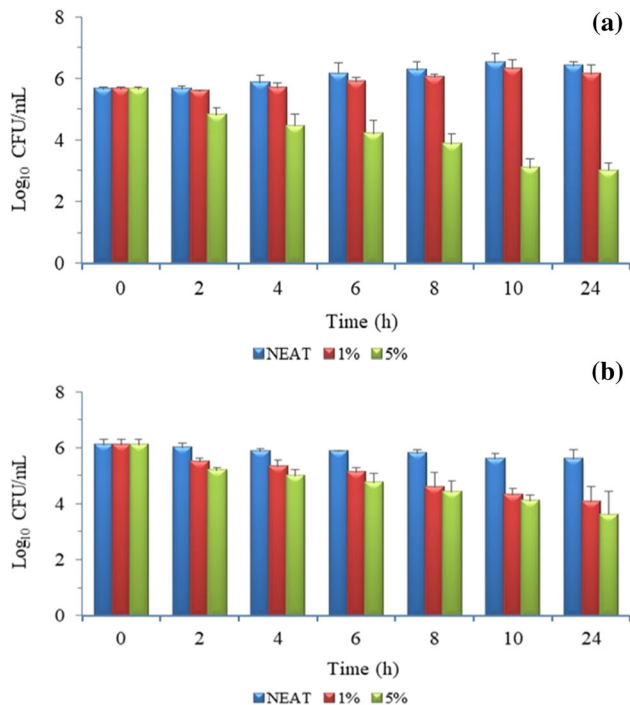
Figure 10 Graphic representation of the CFU/mL values over time of *E. coli* (**a**) and *S. aureus* (**b**) from Pebax® − 1 and 5 wt% Chol-Calix films and neat Pebax® films.

with Pebax® − 5 wt % Chol-Calix that reduced the number of viable *E. coli* cells of 2.57 and 2.66 log CFU/mL (99.7 and 99.8% decrease) at 10 and 24 h, respectively. A similar antibacterial effect was observed against *S. aureus* with a reduction of 2 log CFU/mL (99%) at 10 h that increased to 2.49 log CFU/mL (99.7%) at 24 h.

The higher antibacterial effect against *S. aureus* compared to *E. coli* showed by the film loaded with 1% of Chol-Calix can be explained by the different cell wall structure of these microorganisms and the greater susceptibility of the Gram positive bacteria to quaternary ammonium salts and ammonium-calixarene derivatives [43–45]. Conversely, the similar bactericidal effect shown by the films with 5% loading is likely due to the high amount of Chol-Calix released, which is enough to inhibit both bacteria growth.

Analogously to other polycationic calixarene derivatives [11, 46] the antibacterial activity of Chol-Calix is mainly due to the physical alteration of the bacterial cell membrane. The formation of holes in the outer membrane of Gram-negative bacteria was demonstrated for a polycationic *para*-guanidinoethylcalix[4]arene derivative by atomic force

microscopy images [47]. Charge-to-charge interactions between the positively charged Chol-Calix with the negatively charged bacterial membrane and intercalation of the dodecyl chains of Chol-Calix in the lipophilic membrane moieties alter the bacterial membrane. Moreover, the binding of the choline ligands to choline transporters (BCCT, Betaine-Choline-Carnitine Transporter family) present on the membrane of Gram-negative such as *E. coli* could also be involved in the antibacterial activity of Chol-Calix [18]. It is remarkable that like other antibacterial polycationic calixarene derivatives showing no hemolytic effect and low toxicity toward mammalian cells [11], Chol-Calix exhibited no significant toxicity against different eukaryotic cell lines [12, 15, 48].

To evaluate whether the presence of Chol-Calix can also hinder the formation of biofilm on the surface of the developed Thin-Films, biofilm biomass measurements were performed. Indeed, *E. coli* and *S. aureus* were found to develop on polyamide nanofibers depending on size and morphology [49]. The microbiological tests showed that *E. coli* and *S. aureus* formed a weak biofilm (OD_{492} = 0.14–0.24) on the neat film surface. However, the films containing 5 wt% of Chol-Calix presented a 30–31% reduction in the bacteria biomass compared to that formed on neat polymer matrix. This behavior can be ascribed to the capability of Chol-Calix to reduce the planktonic bacterial load and confer higher hydrophilicity to the film surface, as confirmed by WCA tests.

Attractive aspects of the prepared novel antimicrobial films rely on the use of a biocompatible thermoplastic poly(ether-b-amide) copolymer that is flexible, highly permeable and can be processed using a non-toxic solvent [50].

Cell viability

To investigate the safety of the newly proposed films, we tested the effect of the release from differently loaded films (neat Pebax® and its blend films bearing 0.5%, 1%, or 5% of Chol-Calix) on mouse embryonic fibroblasts NIH/3T3. The potential application of Pebax 2533/Chol-Calix blends as antimicrobial films implies that, at the concentrations used, the amount of compound released does not affect cell viability.

To mimic a physiological condition and test the release of Chol-Calix in a more enriched environment, round films were incubated in the cellular medium DMEM/F12 with 5% FBS, for a time longer
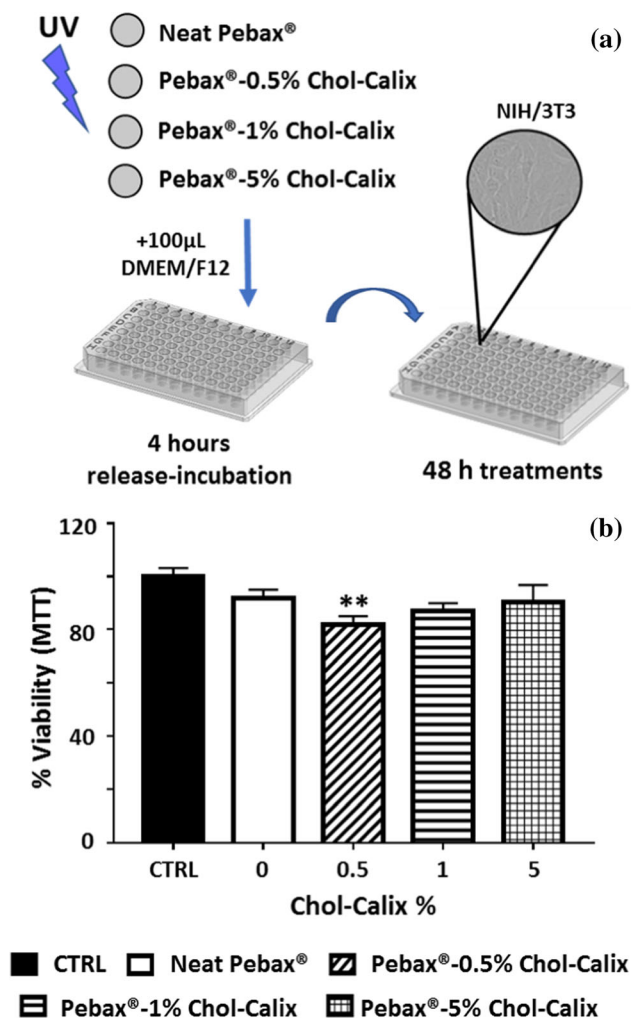
Figure 11 Effects of the release from neat Pebax® and its blend films loaded with 0.5%, 1% or 5% of Chol-Calix, after four hours of incubation in DMEM-F12 medium with 5% FBS. Chol-Calix enriched media were used as treatments on mouse embryonic fibroblast cells (NIH/3T3). (**a**) Scheme of methodology; (**b**) Cell viability assessed by MTT analysis after 48 h treatments. Bars represent means ± Standard Error of Mean (SEM) of three independent experiments with $n = 3$ each. **$*P < 0.05$, vs Ctrl by One-Way ANOVA + Tukey Test.

than 2 h (4 h), according to the release profile previously reported. To test the potential toxicity of Chol-Calix-enriched medium, we used the same condition of release adopted for the antimicrobial test and we treated fibroblasts NIH/3T3 for 48 h to allow the appearance of possible delayed toxicity. As shown in Fig. 11, the cellular viability test used, the MTT assay, revealed that at any conditions of release, Chol-Calix was not toxic (81–90% cell viability range compared to control).

To the best of our knowledge, only a few papers have been published on antibacterial materials based on a Pebax® copolymer. In particular, Ag/Pebax composite nanofibres [51], antibacterial and antifungal breathable Pebax/chloropropane diol membranes [52], antimicrobial Pebax/ILs blends [21], antimicrobial Toluidine Blue O/Pebax extrudates (TBO/Pebax®) [25] have been produced till now. Moreover, only one example of bacteriophilic materials obtained by covalent-linkage of a calixarene-derived to resins [53], and calixarene-embedded membranes for clean water, clean energy production and pharmaceutical separation are present in the literature [54]. Therefore, the obtained Pebax®/Chol-Calix thin-films are the first example of flexible films filled with an antibacterial calixarene derivative. When loaded into Pebax® matrix, Chol-Calix maintains its antibacterial and antibiofilm activity against specimens of Gram-negative and Gram-positive bacteria, responsible for serious infections and does not display cytotoxicity on mouse embryonic fibroblasts NIH/3T3.

According to the experimental results, the idea to develop flexible Thin-Films that can be made with diverse additives, in different sizes and shapes is of great interest for the fabrication of removable drug delivery devices. In this view, Chol-Calix for the already demonstrated capability to load conventional antibiotics [16] and photoactivable molecules [14, 15] in its micellar nanostructure appears appealing for the development of even more effective and photoactivable antibacterial Thin-films.

Conclusions

Chol-Calix, a nanoconstruct obtained by the self-assembly of multiple units of an amphiphilic calix[4]arene derivative bearing choline moieties and dodecyl chains, was synthesized and incorporated in an elastomeric polyether block amide. Flexible free-standing films based on Pebax®2533 loaded with the Chol-Calix nanoconstructs at 0.5, 1 and 5 wt% were prepared by solution casting, utilizing a non-toxic solvent (ethanol), without plasticizers.

The thermal stability of the copolymer matrix is preserved in the blends, while the crystallinity of the copolymer blocks is increased. The presence of the additive can be observed on the film surface, according to its concentration in the matrix. The wettability of the films increases upon the Chol-Calix

loading in the blend membranes. Low content of Chol-Calix slightly reduces the gas permeability through the films, whereas an increase in this parameter is observed as Chol-Calix amount rises, due to the additive aggregation tendency.

Low leaching of Chol-Calix from the film surface was confirmed through release tests carried out in PBS medium. The blend films displayed antimicrobial activity within 10 h against Gram-negative (*E. coli*) and Gram-positive (*S. aureus*) bacteria that represent clinically important strains. In addition, the Chol-Calix was capable to interfere with the biofilm formation since the films loaded with the higher concentration of Chol-Calix demonstrated a one-third reduction in biofilm formation on their surface. Furthermore, the blend films did not exert cytotoxicity on mouse embryonic fibroblasts NIH/3T3.

The obtained results suggest the Pebax2533/Chol-Calix combination as a promising approach for the development of novel flexible antibacterial Thin-films that could be upgraded by loading antibacterial drugs in the Chol-Calix nanocarrier.

Acknowledgements

References

[1] Muñoz-Bonilla A, Echeverria C, Sonseca Á, Arrieta MP, Fernández-García M (2019) Bio-based polymers with antimicrobial properties towards sustainable development. Materials 12:641–683. https://doi.org/10.3390/ma12040641

[2] Gao L, Wang H, Zheng B, Huang F (2021) Combating antibiotic resistance: Current strategies for the discovery of novel antibacterial materials based on macrocycle supramolecular chemistry. Giant 7:100066. https://doi.org/10.1016/j.giant.2021.100066

[3] Böhmer V (1995) Calixarenes, macrocycles with (almost) unlimited possibilities. Angew Chem Int Ed Engl 34:713–745. https://doi.org/10.1002/anie.199507131

[4] Wei A (2006) Calixarene-encapsulated nanoparticles: self-assembly into functional nanomaterials. Chem Commun 15:1581–1591. https://doi.org/10.1039/B515806K

[5] Hussain MA, Ashraf MU, Muhammad G, Tahir MN, Bukhari SNA (2017) Calixarene: a versatile material for drug design and applications. Curr Pharm Des 23:2377–2388. https://doi.org/10.2174/1381612822666160928143328

[6] Renziehausen A, Tsiailanis AD, Perryman R, Stylos EK, Chatzigiannis C, O'Neill K et al (2019) Encapsulation of temozolomide in a calixarene nanocapsule improves its stability and enhances its therapeutic efficacy against glioblastoma. Mol Cancer Ther 18:1497–1505. https://doi.org/10.1158/1535-7163.MCT-18-1250

[7] Shurpik DN, Padnya PL, Stoikov II, Cragg PJ (2020) Antimicrobial activity of calixarenes and related macrocycles. Molecules 25:5145. https://doi.org/10.3390/molecules25215145

[8] Colston MJ, Hailes HC, Stavropoulos E (2004) Antimycobacterial calixarenes enhance innate defense mechanisms in murine macrophages and induce control of mycobacterium tuberculosis infection in mice. Infect Immun 11:6318–6323. https://doi.org/10.1128/IAI.72.11.6318-6323.2004

[9] Basilotta R, Mannino D, Filippone A et al (2021) Role of calixarene in chemotherapy delivery strategies. Molecules 26:3963. https://doi.org/10.3390/molecules26133963

[10] Fang S, Dang Y-Y, Li H et al (2022) Membrane-active antibacterial agents based on calix[4]arene derivatives: synthesis and biological evaluation. Front Chem 10:816741. https://doi.org/10.3389/fchem.2022.816741

[11] Rodik RV, Anthony A-S, Kalchenko VI, Mély Y, Klymchenko AS (2015) Cationic amphiphilic calixarenes to compact DNA into small nanoparticles for gene delivery. New J Chem 39:1654–1664. https://doi.org/10.1039/C4NJ01395F

[12] Granata G, Paterniti I, Geraci C et al (2017) Potential eye drop based on a calix[4]arene nanoassembly for curcumin delivery: enhanced drug solubility, stability, and anti-inflammatory effect. Mol Pharm 14:1610–1622. https://doi.org/10.1021/acs.molpharmaceut.6b01066

[13] Granata G, Petralia S, Forte G, Conoci S, Consoli GML (2020) Injectable supramolecular nanohydrogel from a micellar self-assembling calix [4] arene derivative and curcumin for a sustained drug release. Mater Sci Eng C 111:110842. https://doi.org/10.1016/j.msec.2020.110842

[14] Di Bari I, Fraix A, Picciotto R et al (2016) Supramolecular activation of the photodynamic properties of porphyrinoid photosensitizers by calix [4]arene nanoassemblies. RSC Adv 6:105573–105577. https://doi.org/10.1039/C6RA23492E

[15] Di Bari I, Picciotto R, Granata G, Blanco AR, Consoli GML, Sortino S (2016) A bactericidal calix[4]arene-based nanoconstruct with amplified NO photorelease. Org Biomol Chem 14:8047–8052. https://doi.org/10.1039/C6OB01305H

[16] Migliore R, Granata G, Rivoli A, Consoli GML, Sgarlata C (2021) Binding affinity and driving forces for the interaction of calixarene-based micellar aggregates with model antibiotics in neutral aqueous solution. Front Chem 8:626467. https://doi.org/10.3389/fchem.2020.626467

[17] Consoli GML, Granata G, Ginestra G, Marino A, Toscano G, Nostro A (2022) Antibacterial nanoassembled calix[4]-arene with exposed choline units inhibits biofilm formation and motility of gram negative bacteria. ACS Med Chem Lett 13:916–922. https://doi.org/10.1021/acsmedchemlett.2c00015

[18] Karki S, Kim H, Na S-J, Shin D, Jo K, Lee J (2016) Thin films as an emerging platform for drug delivery. Asian J Pharm Sci 11:559–574. https://doi.org/10.1016/j.ajps.2016.05.004

[19] Crick CR, Noimark S, Peveler WJ, Bear JC, Ivanov AP, Edel JB, Parkin IP (2015) Advanced analysis of nanoparticle composites - a means toward increasing the efficiency of functional materials. RSC Adv 5:53789–53795. https://doi.org/10.1039/C5RA08788K

[20] Bernardo P, Jansen JC, Bazzarelli F et al (2012) Gas transport properties of PEBAX®/room temperature Ionic liquid gel membranes. Sep Purif Tech 97:73–82. https://doi.org/10.1016/j.seppur.2012.02.041

[21] Clarizia G, Bernardo P, Carroccio SC, Ussia M, Restuccia C, Parafati L, Calarco A, Zampino D (2020) Heterogenized Imidazolium-based ionic liquids in Pebax®RNew. Therm Gas Transp Antimicrob Prop Polym 12:1419–1437. https://doi.org/10.3390/polym12061419

[22] McKeen LW (2015) Thermoplastic elastomers. The effect of creep and other time related factors on plastics and elastomers. Elsevier, pp 355–372. https://doi.org/10.1016/B978-0-323-35313-7.00008-0

[23] Jiang X, Liang S, Wang F, Geng W (2015) Electrospun functional poly(ether amide) composite nanofibres. TechConnect Briefs 3:293–296

[24] Sole BB, Lohkna S, Chhabra PK, Prakash V, Seshadri G, Tyagi AK (2018) Preparation of mechanically strong poly (ether block amide)/mercaptoethanol breathable membranes for biomedical applications. J Polym Res 25:200. https://doi.org/10.1007/s10965-018-1596-1

[25] Wylie MP, Irwin NJ, Howard D, Heydon K, McCoy CP (2021) Hot-melt extrusion of photodynamic antimicrobial polymers for prevention of microbial contamination. J Photochem Photobiol B: Biology 214:112098. https://doi.org/10.1016/j.jphotobiol.2020.112098

[26] Yang O, Kim HL, Weon J-I, Seo YR (2015) Endocrine-disrupting chemicals: review of toxicological mechanisms using molecular pathway analysis. J Cancer Prev 20:12–24. https://doi.org/10.15430/JCP.2015.20.1.12

[27] Fanelli R, Zuccato E (2002) Risks and benefits of PVC in medical applications. Boll Chim Farm 141:282–289

[28] Clarizia G, Bernardo P, Gorrasi G, Zampino D, Carroccio SC (2018) Influence of the preparation method and photo-oxidation treatment on the thermal and gas transport properties of dense films based on a poly(ether-block-amide) copolymer. Materials 11:1326–1334. https://doi.org/10.3390/ma11081326

[29] Eggers PK, Becker T, Melvin MK et al (2012) Composite fluorescent vesicles based on ionic and cationic amphiphilic calix[4]arenes. RSC Adv 2:6250–6257. https://doi.org/10.1039/C2RA20491F

[30] Tekin K, Hao N, Karagoz S, Ragauskas AJ (2018) Ethanol: a promising green solvent for the deconstruction of lignocellulose. Chem Sus Chem 11:3559–3565. https://doi.org/10.1002/cssc.201801291

[31] Crank J (1975) The mathematics of diffusion, 2nd edn. Clarendon Press, Oxford

[32] Wijmans JG, Baker RW (1995) The solution-diffusion model: a review. J Membr Sci 107:1–21. https://doi.org/10.1016/0376-7388(95)00102-I

[33] Cascone S (2017) Modeling and comparison of release profiles: effect of the dissolution method. Eur J Pharm Sci 106:352–361. https://doi.org/10.1016/j.ejps.2017.06.021

[34] Nostro A, Sudano Roccaro A, Bisignano G et al (2007) Effects of oregano, carvacrol and thymol on staphylococcus aureus and staphylococcus epidermidis biofilms. J Med

Microbiol 56:519–523. https://doi.org/10.1099/jmm.0.46804-0

[35] Beiragh HH, Omidkhah M, Abedini R, Khosravi T, Pakseresht S (2016) Synthesis and characterization of poly (ether-block-amide) mixed matrix membranes incorporated by nanoporous ZSM-5 particles for CO_2/CH_4 separation. Asia-Pac J Chem Eng 11:522–532. https://doi.org/10.1002/apj.1973

[36] Vieira L, Schenna R, Gollas B (2015) In situ PM-IRRAS of a glassy carbon electrode/deep eutectic solvent interface. Phys Chem Chem Phys 17:12870–12880. https://doi.org/10.1039/C5CP00070J

[37] Sheth JP, Xu J, Wilkes GL (2003) Solid state structure–property behavior of semicrystalline poly(ether-block-amide) PEBAX® thermoplastic elastomers. Polymer 44:743–756. https://doi.org/10.1016/S0032-3861(02)00798-X

[38] Maxwell JC (2010) A treatise on electricity and magnetism. Cambridge University Press

[39] Bernardo P, Clarizia G (2022) A review of the recent progress in the development of Nanocomposites based on poly(ether-block-amide) copolymers as membranes for CO_2 separation. Polymers 14:10. https://doi.org/10.3390/polym14010010

[40] Zampino D, Mancuso M, Zaccone R et al (2021) Thermo-mechanical, antimicrobial and biocompatible properties of PVC blends based on imidazolium ionic liquids. Mater Sci Eng C 122:111920. https://doi.org/10.1016/j.msec.2021.111920

[41] Balcerzak J, Mucha M (2010) Analysis of model drug release kinetics from complex matrices of polylactide-chitosan. Progr Chem Appl Chitin Deriv 15:117–126

[42] Cerca N, Pier GB, Vilanova M, Oliveira R, Azeredo J (2005) Quantitative analysis of adhesion and biofilm formation on hydrophilic and hydrophobic surfaces of clinical isolates of Staphylococcus epidermidis. Res Microbiol 156:506–514. https://doi.org/10.1016/j.resmic.2005.01.007

[43] Bragg R, Jansen A, Coetzee M, van der Westhuizen W, Boucher C (2014) Bacterial resistance to quaternary ammonium compounds (QAC) disinfectants. Adv Exp Med Biol 808:1–13. https://doi.org/10.1007/978-81-322-1774-9_1

[44] Consoli GML, Granata G, Picciotto R, Blanco AR, Geraci C, Marino A, Nostro A (2018) Design, synthesis and antibacterial evaluation of a polycationic calix[4]arene derivative alone and in combination with antibiotics. Med Chem Commun 9:160–164. https://doi.org/10.1039/C7MD00527J

[45] Consoli GML, Di Bari I, Blanco AR, Nostro A, D'Arrigo M, Pistarà V, Sortino S (2017) Design, synthesis, and antibacterial activity of a multivalent polycationic Calix[4]arene-NO photodonor conjugate. ACS Med Chem Lett 8(8):881–885. https://doi.org/10.1021/acsmedchemlett.7b00228

[46] Formosa C, Grare M, Jauvert E, Coutable A, Regnouf-de-Vains J-B, Mourer M, Duval RE, Dague E (2012) Nanoscale analysis of effects of antibiotics and CX1 on a *Pseudomonas aeruginosa* multidrug-resistant strains. Sci Rep 2(575):1–9. https://doi.org/10.1038/srep00575

[47] Sautrey G, Orlof M, Korchowiec B, Regnouf de Vains J-B, Rog E (2011) Membrane activity of tetra-p-guanidinoethyl-calix[4]arene as a possible reason for its antibacterial properties. Phys Chem B 115:15002–15012. https://doi.org/10.1021/jp208970g

[48] Blanco AR, Bondì ML, Cavallaro G et al (2016) Nanostructured formulations for the delivery of silibinin and other active ingredients for treating ocular diseases. WO/2016/055976. https://patentimages.storage.googleapis.com/cf/4c/7e/caed13f05133fc/WO2016055976A1.pdf. Accessed 22 July 2022

[49] Lencova S, Svarcova V, Stiborova H, Demnerova K, Jencova V, Hozdova K, Zdenkova K (2021) Bacterial biofilms on polyamide nanofibers: factors influencing biofilm formation and evaluation. ACS Appl Mater Interfaces 13:2277–2288. https://doi.org/10.1021/acsami.0c19016

[50] Capello C, Fischer U, Hungerbühler K (2007) What is a green solvent? A comprehensive framework for the environmental assessment of solvents. Green Chem 9:927–934. https://doi.org/10.1039/B617536H

[51] Liang S, Zhang G, Min J, Ding J, Jiang X (2014) Synthesis and antibacterial testing of silver/poly (ether amide) composite nanofibers with ultralow silver content. J Nanomater Article ID 684251:1–10. https://doi.org/10.1155/2014/684251

[52] Sole BB, Seshadri G, Tyagi AK, Rattan S (2018) Preparation of antibacterial and antifungal breathable polyether block amide/chloropropane diol membranes via- solution casting. J Appl Polym Sci 46097:1–9. https://doi.org/10.1002/APP.46097

[53] Lemée F, Mourer M, Aranda L, Clarot I, Regnouf-de-Vains J-B (2016) Bacteriophilic tetra-p-guanidinoethyl-calix[4]arene derived polymers. Syntheses and E. coli sequestration studies. New J Chem 40:8239–8250. https://doi.org/10.1039/C6NJ01563H

[54] Chung T-S, Lai J-Y (2022) The potential of calixarenes for membrane separation. Chem Eng Res Des 183:538–545. https://doi.org/10.1016/j.cherd.2022.05.031

⚫ Springer